DOI: http://dx.doi.org/10.21123/bsj.2019.16.3(Suppl.).0726

Geometry, and Normal Modes of Vibration (3N-6) for Di and Tetra-Rings Layer (6, 0) Linear (Zigzag) SWCNTs; A DFT Treatment

Rehab M. Kubba * ***Khalida A. Samawi***

Received 3/8/2018, Accepted 3/4/2019, Published 22/9/2019

Abstract:

Density Functional Theory (DFT) method of the type (B3LYP) and a Gaussian basis set (6-311G) were applied for calculating the vibration frequencies and absorption intensities for normal coordinates (3N-6) at the equilibrium geometry of the Di and Tetra-rings layer (6, 0) zigzag single wall carbon nanotubes (SWCNTs) by using Gaussian-09 program. Both were found to have the same symmetry of D_{6d} point group with C--C bond alternation in all tube rings (for axial bonds, which are the vertical C--Ca bonds in rings layer and for circumferential bonds C—Cc in the outer and mid rings bonds). Assignments of the modes of vibration IR active and inactive vibration frequencies (symmetric and asymmetric modes) based on the image modes applied by the Gaussian 09 display. The whole relations for the vibration modes were also done including νCH stretching, νC--C stretching, δCH, δring (δC--C--C) deformation in plane of the molecule) and γCH, γring (γC--C--C) deformation out of plane of the molecule. The assignment also included modes of puckering, breathing and clock-anticlockwise bending vibrations.

Key word: Di and Tetra-rings Layer, IR Absorption Intensities, Modes of vibration, Normal coordinates, SWCNT, Vibration frequencies.

Introduction:

The vibration behavior of carbon nanotubes (CNTs) has been extensively investigated due to their importance in Nano-electro-mechanical systems and Nano sensor application. Raman spectroscopy is a technique widely used to study the vibrational modes of CNTs and characterize their structures. The Raman spectrum analysis focuses on the low-frequency radial breathing modes with less than 300 cm^{-1}, which are very sensitive to the nanotube diameters (1-4).Since experiments at the Nano scale are extremely difficult to conduct, theoretical modeling of the mechanical response of CNTs has been carried out (5,6). They are shown graphically and have been compared with those available in the literature. Vibration characteristics of CNTs have been widely examined for the last fifteen years. Such characteristics are studied by thin shell (7), beam (8) and ring (9) theories of continuum models (10). Theoretical study of CNTs reflects those mechanical aspects which are difficult to observe by experimental and atomistic simulation methodologies. A study of their free vibration is an important phenomenon in dynamical science. These characteristics are impressed by their material properties.

Department of Chemistry, College of Science, University of Baghdad, Baghdad, Iraq.
*Corresponding author: Rehab_mmr_kb@yahoo.com

These tubes are placed in various physical environments and subject to various constraints. Influence of these constraints is investigated on vibration characteristics of single-walled carbon nanotubes (SWCNTs). Carbon nanotubes (CNTs) have a vast field of applicationsin material strength analysis. Some worth-mentioning fields are emanation panel spectacle, chemical sensing, drug deliverance, and Nano-electronics. Having a good utilization of these tubes in fields of science and industry, however, their mechanical behavior demands more understanding in this aspect of study. Use of these tubes had found in the fields of electrical and chemical engineering and biological sciences. An experimental aspect of vibration problems of (SWCNTs) have also been interest of researchers along with analytical study of information got through it. Three fundamental techniques are utilized to generate them, which include molecular dynamic (MD) simulations, atomistic-based modeling and the continuum approach. Mostly the continuum method is applied to fabricate them. Since these are material objects can get deformed in practical situations, so their buckling and vibration investigations are fundamental problems in CNTs motions at non-mechanical levels. Lordi and Yao (11) applied molecular dynamic simulations todetermine

vibration frequencies of SWCNTs using the universal force field method.

In the recent studies we calculated and studied theoretically, the complete assignments for vibration frequencies and absorption intensities of (3N-6) for monoring segments of CNTs (linear, angular and angular-chiral) (12,13) and for the (6,0) linear (zigzag Tri-rings layer) SWCNT. Comparisons were done for the vibration frequencies of monoring SWCNTs with different diameters (14), for construction units of (6,0) (15) armchair and zigzag SWCNTs (16). In this work, the theoretical calculations of the Density Functional Theory quantum mechanical method (DFT) (17), is applied, in the form of the B3LYP approach (18-19) and the 6-311G Gaussian bases set (20) is used, for calculating vibration frequencies and normal modes of vibration (3N-6) for Di and Tetra-rings layer (6, 0) linear (zigzag) SWCNTs

Computational Details

DFT (6-311G/ B3LYP) calculations were performed with complete geometrical optimization, for Di and Tetra-RL (6, 0) linear (zigzag) SWCNTs using Gaussian-09 software package (21). The calculations were used to analyze and describe the characteristics of the structural nature of the modes of vibration with IR absorption intensities for Di and Tetra-rings layer zigzag SWCNTs.

Results and Discussion:

The classifications of carbon nanotubes Di and Tetra-rings layers can be described as SWNTs resembling rolling graphene sheet into a cylindrical structure.They are uniquely defined by specifying the coordinates of the smallest folding vector (n, 0) linear zigzag SWCNTs (22), composing of linear numbers of benzene ring molecules. So Di and Tetra rings layer SWCNTs are composed of linear six members of benzene aromatic rings in each of the two or four rings layer respectively. DFT (B3LYP/6-311G) calculations of the equilibrium geometries, shows D_{6d} symmetry point group for both (23). The geometric parameters were defined, distinguished between axial bonds (C--Ca), outer, and mid circumferential bonds (C--Cc). Figure 1, shows the space filling; minimize geometry and repetitive sections of the two types of bonds in Di and Tetra-rings layer zigzag CNTs due to their D_{6d} symmetry.

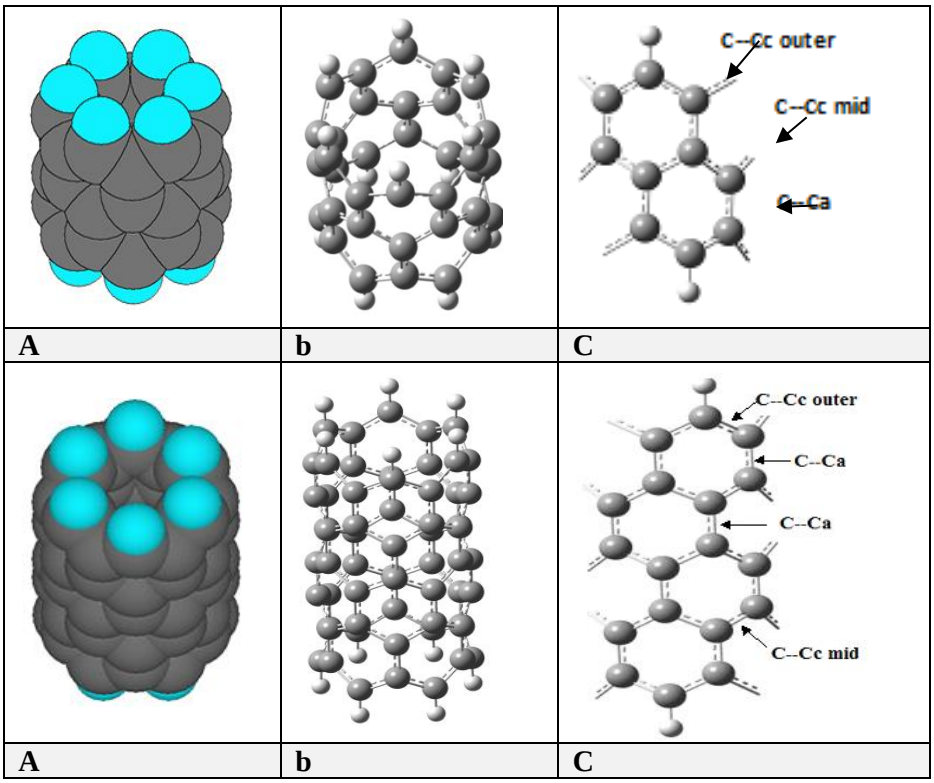

Figure 1. The space filling (a), minimize geometry (b), repetitive sections of bonds and angles for Di and Tetra-rings-layer (6, 0) zigzag (SWCNTs) according to the D_{6d} point group (c).

All C-C bonds were found to be alternated in the rings tube according to D_{6d} point group. The C-C bonds at the optimize zigzag Di-rings-layer SWCNTs were all being as conjugated double bonds.Tables 1a, 1b show that (C--Cc) bonds length for both Di and Tetra-rings layer SWCNT were being longer (weaker with lower force constant) on going from outer to mid bonds in Di rings layer or

on going to center bonds in (Tetra rings layer). The (the reverse were shown for the axial bonds (C--Ca)(12,15-16). Also the Gaussian 09 program have been employed to computesome physical properties such as a standard heat of formation ΔH_f, dipole moment μ which is equal to zero Debye, the HOMO (Highest Occupied Molecular Orbital) and LUMO (Lowest Unoccupied Molecular Orbital). E_{HOMO} is often associated with the ability of donating electrons. High values of E_{HOMO} likely indicate a tendency for donating electrons to appropriate acceptors with low energy and empty molecular orbital. Similarly, E_{LUMO} represents the ability of the molecule to accept electrons. The lower value of E_{LUMO} suggests high probability for accepting electrons (12). The low value of $\Delta E_{HOMO-LUMO}$ leads to ensure better physical properties of electrical conductivity (15-16, 24-25). Figure 2, shows the numbering of the atoms of (6, 0) Di and Tetra-ring layers (zigzag) SWCNTs respectively.

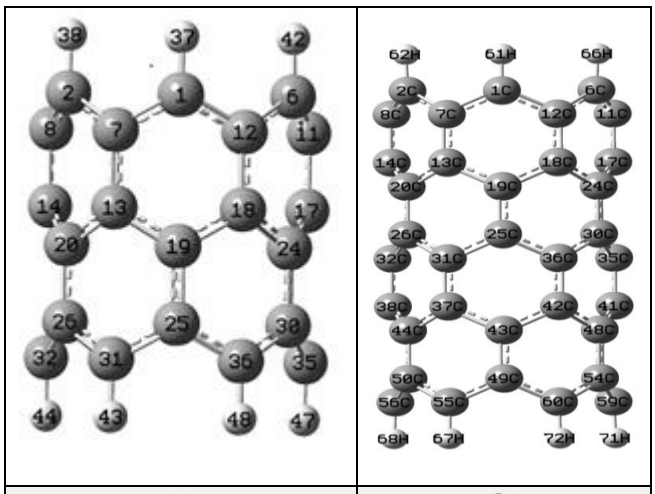

(a) **(b)**

Figure 2. Numbering of atoms for (6, 0) Di (a) and (b) Tetra-rings layer (zigzag) SWCNT.

The calculation of the geometric structures and some physical properties for the Di and Tetra-rings layer SWCNT at the equilibrium geometry, are listed in Tables 1a, 1b respectively.

Table 1a. DFT calculations for the geometrical structure and some physical properties of the Di-rings-layer SWCNT.

Bond lengths (A^0) & bond angles (deg.)		Physical properties	
C1-C7 (C-Cc) outer	1.425	Molecular formula	$C_{36}H_{12}$
C7-C13 (C-Ca) axial	1.448	M.wt. (g/mol.)	444.491
C13-C20 (C-Cc) mid	1.432	ΔH_f (kcal/mol)	532.942
C1-H37	1.083	Electronic energy (eV)	-48491.023
< C7C1C12	115.529	Core-core repulsion (eV)	44059.087
< C1C7H13	118.462	Ionization potential (eV)	4.633
< H1C12C6	116.814	E_{HOMO} (eV)	-4.633
< C13C19C18	114.349	E_{LUMO} (eV)	-2.793
< C7C1H37	118.265	$\Delta E_{HOMO-LUMO}$ (eV)	1.84
--------	--------	Dipole moment (Debye)	0.000

Table 1b. DFT calculations for the geometrical structure and some physical properties of the Tetra rings-layer SWCNT.

Bond lengths (A^0) & bond angles (deg.)		Physical properties	
C1-C7 (C-Cc) outer	1.427	Molecular formula	$C_{60}H_{12}$
C7-C13 (C-Ca) outer	1.433	m. wt. (g/mol.)	732.755
C13-C19 (C-Cc) mid.	1.444	Point group	D_{6d}
C19-C25 (C-Ca) mid.	1.420	ΔH_f (kJ/ mol)	2945.663
C25-C36 (C-Ca) mid.	1.446	Electronic energy (eV)	590749.199
C1-H61	1.083	Core-core repulsion (eV)	229970.081
< C7C1C12	116.019	Ionization potential (eV)	3.822
< C1C7C13	119.329	E_{HOMO} (eV)	-3.822
< C7C13C19	119.593	E_{LUMO} (eV)	-3.384
< C13C19C18	114.171	$\Delta E_{HOMO-LUMO}$ (eV)	0.438
< C19C13C20	114.249	Dipole moment (Debye)	0.000
< C20C26C31	119.691	-------	-------
< C31C25H36	114.068	-------	-------
< C7C1H61	119.708	-------	-------

$\Delta E_g = E_{LUMO} - E_{HOMO}$.

The finger print vibrations (basic vibrations) of Di and Tetra-rings layer (Di and Tetra-RL) SWCNTs were calculated and assigned such as breathing, puckering, elongation and clock-anti-clockwise bending or deformation modes. Active vibrations cause a change in its geometric structure. Measurements were made to study the effect of curvature distortion on the electronic properties of carbon nanotubes (26-29).

For a normal mode of vibration to be active in infrared, there must be a change in the dipole moment of the molecule during the vibration process (during the vibration motion of a molecule, a regular fluctuation occurs in the dipole moment, and the established fieldcan interact with the radiation-related electric field). In order to absorb the infrared, radiation, a molecule must undergo a net change in its dipole moment due to its own vibration movements (30).

Vibration Frequencies and Absorption Intensities of the Calculated SWCNTs

Geometrical optimizations have been performed at the calculations of (DFT/B3LYP) to evaluate the vibration frequencies and Infra-Red (IR) absorption intensities for of (6,0) zigzag Di and Tetra-RL.

Equilibrium geometry of (D_{6d}) point group makes the (6,0) Di andTetra-rings layer zigzag SWCNT undergo 24 symmetry operations **(E, $2S_{12}$, $2C_6$, $2S_4$, $2C_3$, $2S^5_{12}$, C_2, $6C'_6$, $6\sigma_d$)** (23, 30).

-Vibration Frequencies Assignment of Di-Rings Layer (6, 0) Zigzag SWCNT

The Di-RL zigzag SWCNT posses 138 fundamental vibrations. Inspection of its irreducible representations, as defined by the symmetry character table (23), results in the following modes of vibration;

$\Gamma_{vibration}= \Gamma_{total}- (\Gamma_{rotation}+ \Gamma_{translation}) = 3N-6= 3x48-6= 144-6= 138=8A_1+ 4B_1+ 3A_2+ 7B_2+ 11E_1 + 12E_2+ 12E_3+ 12E_4+ 11E_5$

- Symmetric to the Plane (of the Molecule)

There are 18 **IR active** modes of vibration ($7B_2$+ $11E_1$), and 31**Raman active**modes of vibration ($8A_1$ (polarized) +$12E_2$ (depolarized)+$11E_5$ (depolarized) (22, 25), can be assigned as follows:

- νCH Stretching Vibrations

These are 12 CH stretching vibrations according to number of (CH) bonds. The range of frequency values is (3028-3041cm^{-1}), showing the following correlation:

ν_{sym} CH str.(3041 cm^{-1}) (A_1)> ν_{asym}CH str. (3040 cm^{-1}) (B_2)

The highest intensity is **120.444 km/mol** due to ν_{16}(3040 cm^{-1}) (B_2).

- ν(C--C) Stretching Vibrations

The range of the calculated (C--C) stretching vibration frequencies is (1323-1555 cm^{-1}), shown in the following relations;

$\nu_{sym.}$(C--C str.)(1555 cm^{-1})(axial.)(A_1)>$\nu_{asym.}$(C--C str.)(1525 cm^{-1})(axial.)(E_1)

$\nu_{sym.}$(C--C str.)(1555 cm^{-1})(axial.)(A_1)>$\nu_{asym.}$(C--C str.)(1513 cm^{-1})(circum.)(E_5)

In general:**$\nu_{sym.}$ (C--C str.) >$\nu_{asym.}$ (C--Cstr.)**

- νRing (C--C--C) Stretching Vibrations

The vibration of these modesare not located at definite C atoms like **ν(CC)**as could be seen from the atomic displacement vectors. According to their assignment, they fall in the range of (1198-1468 cm^{-1}).

$\nu_{asym.}$(C--C--C str.) (1468 cm^{-1}) (axial.) (B_2)>$\nu_{asym.}$(C--C--C str.)(1360 cm^{-1})(circum.)(E_3)

The highest intensity is **4.299 km/mol** for ν_{17} (1468cm^{-1}) (B_2).

- δCH in-Plane (of the tube) CH DeformationVibrations

Their displacement vectors are mainly located at the corresponding H atoms. The range of the calculated frequency values is (1152-1440 cm^{-1}).

$(\delta CH)_{asym}$ scissoring (1440cm^{-1}) (E_3)> $(\delta CH)_{asym}$ (clock-anticlockwise) (rocking) (1418cm^{-1}) (A_2)

The highest intensity is **16.451km/mol** due to $\nu_{27,28}$ (1367 cm^{-1}) (E_1).

- In Plane (of the Tube) Deformation Vibrations (δC--C--C)

The deformation of smaller values is (δ**C--C--C**) vibrations. According to their assignment, they were fallen in the range of (328-1302 cm^{-1}). These modes include the expected clock and anticlockwise vibration motions, also showing the following relations;

$(\delta C\text{--}C\text{--}C)_{sym.}$(elongation) (1302 cm^{-1}) (A_1) > $(\delta C\text{--}C\text{--}C)_{asym.}$(circum.) (1262 cm^{-1})(E_1)

The highest intensity is **34.914km/mol** for ν_{21} (580 cm^{-1}) (B_2).

- Out of Plane (of the Tube) Deformation Vibration Frequencies (γCH)

The range of the (γCH) out of plane vibrations frequency is (436-931cm^{-1}). The following relations hold to;

$(\gamma CH)_{asym}$ (931cm^{-1}) (wagging) (B_2) > $(\gamma CH)_{asym}$ (928 cm^{-1}) (wagging) (A_1)

$(\gamma CH)_{asym}$ (931cm^{-1}) (wagging) (B_2) > $(\gamma CH)_{asym}$ (867 cm^{-1}) (twisting) (E_2)

The highest intensity is **391.477km/mol** due to $\nu_{33,34}$ (894 cm^{-1}) (E_1).

- γRing Out of Plane (of the Tube) Deformation Vibrations (γC--C--C)

The range of the vibrations frequency values for the ring out of plane (γ**C--C--C**) is (144-995 cm^{-1}). The modes include deformations, puckering as well as breathing vibrations of the whole ring. The relation of the asymmetric to the symmetric modes for the zigzag molecule is viewed in the following relation;

$(\gamma C\text{--}C\text{--}C)_{asym.}$(puck.) (995 cm^{-1}) (E_2)> $(\gamma C\text{--}C\text{--}C)_{sym.}$ (breath.) (750 cm^{-1}) (A_1)

The highest intensity is **83.668km/mol** due to $\nu_{35,\,36}$ (797 cm^{-1}) (E_1).

Table 2, shows the assignment of (3N-6) vibration frequencies and IR active absorption intensities of the Di-RL (6, 0) zigzag SWCNT. Figure 3, shows the IR spectrum of the Di-RL SWCNT as calculated by DFT method. Figure 4 shows the images of some modes of vibration for Di-RL SWCNT.

Table 2. Vibration frequencies assignment of (3N-6) and absorption intensities of the active IR modes for the Di-RL (6,0) zigzag SWCNT.

	Symmetry & description	DFT (6-311G/ B3LYP) Freq. (cm^{-1})	Intensity (km/mol)
A_1			
ν_1	CH str.	3041.32	0.000
ν_2	ring (CC str.)(axial)	1555.02	0.000
ν_3	δring (δCCC) elongation	1301.52	0.000
ν_4	γCH (wagging)	928.21	0.000
ν_5	γring (γCCC) breathing	749.83	0.000
ν_6	δring (δCCC) elongation	548.30	0.000
ν_7	γring (γCCC) breathing	468.15	0.000
ν_8	γring (γCCC) external edge (puckering)	430.31	0.000
B_1			
ν_9	ring (CC str.) (circumference) + δCH clock-anti clock	1460.42	0.000
ν_{10}	ring (CC str.) (circumference) + δCH	1335.11	0.000
ν_{11}	δCH (rocking)	1179.69	0.000
ν_{12}	δring (δCCC) clock-anti clock	327.60	0.000
A_2			
ν_{13}	δH clock-anti clock (rocking)	1418.05	0.000
ν_{14}	δH clock-anti clock (rocking)	1181.57	0.000
ν_{15}	δring (δCCC) clock-anti clock	561.09	0.000
B_2			
ν_{16}	CH str.	3040.27	**120.444**
ν_{17}	ring (CCC str.) (axial)	1468.06	4.299
ν_{18}	δring (δCCC) elongation	982.90	0.144
ν_{19}	γCH (wagging)	931.42	**238.655**
ν_{20}	γring (γCCC) (puckering) axial	701.02	27.138
ν_{21}	δring (δCCC) elongation	580.41	34.914
ν_{22}	γCH (wagging)	436.15	4.194
E_1			
$\nu_{23,\,24}$	CH str.	3036.42	19.391
$\nu_{25,\,26}$	ring (CC str.) (axial) + δCH	1525.31	1.101
$\nu_{27,\,28}$	δCH (rocking)	1366.78	16.451
$\nu_{29,\,30}$	δring (δCCC) circumference	1261.86	4.206
$\nu_{31,\,32}$	δCH (rocking) + δring (δCCC)	1154.48	1.222
$\nu_{33,\,34}$	γCH (wagging)	894.44	**391.477**
$\nu_{35,\,36}$	γring (γCCC) (puckering) circumference	797.08	**83.667**
$\nu_{37,\,38}$	γring (γCCC) puckering (circumference)	681.10	4.812
$\nu_{39,\,40}$	γring (γCCC) puckering (circumference)	603.02	22.013
$\nu_{41,\,42}$	γring (γCCC) (puckering) circumference	485.34	0.053
$\nu_{43,\,44}$	γring (γCCC) puckering (circumference)	312.42	0.002
E_2			

$\nu_{45, 46}$	δCH (scissoring) + ring (CC str.)(axial)	1495.19	0.000
$\nu_{47, 48}$	ring (CCC str.)	1370.78	0.000
$\nu_{49, 50}$	δCH (scissoring)	1281.73	0.000
$\nu_{51, 52}$	ring(CCCstr.) (circumference)	1198.02	0.000
$\nu_{53, 54}$	γring (γCCC) (puckering)	994.60	0.000
$\nu_{55, 56}$	γCH (twist.)	866.74	0.000
$\nu_{57, 58}$	γCH (twist.)	780.40	0.000
$\nu_{59, 60}$	γring (γCCC) (puckering.)	635.02	0.000
$\nu_{61, 62}$	γring (γCCC) (puckering.)	501.47	0.000
$\nu_{63, 64}$	γring (γCCC) (puckering.)	429.99	0.000
$\nu_{65, 66}$	γring (γCCC) (puckering.)	313.58	0.000
$\nu_{67, 68}$	γring (γCCC) (puckering.)	144.30	0.000
E_3			
$\nu_{69,70}$	CH str.	3028.26	0.000
$\nu_{71,72}$	δCH (scissoring)	1439.92	0.000
$\nu_{73,74}$	ring (CCC str.) (circumference)	1359.87	0.000
$\nu_{75,76}$	ring (CCC str.)	1328.79	0.000
$\nu_{77,78}$	ring (CCC str.) (circumference)	1267.64	0.000
$\nu_{79,80}$	δring (δCCC) + δCH (scissoring)	1061.53	0.000
$\nu_{81,82}$	γCH (twisting.)	849.01	0.000
$\nu_{83,84}$	γring (γCCC) (puckering) external edge	716.09	0.000
$\nu_{85,86}$	γring (γCCC) (puckering.)	677.53	0.000
$\nu_{87,88}$	δring (δCCC)	540.47	0.000
$\nu_{89,90}$	γring (γCCC) (puckering.) axial	363.79	0.000
$\nu_{91,92}$	γring (γCCC) (puckering.) external edge	272.46	0.000
E_4			
$\nu_{93,94}$	CH str.	3036.14	0.000
$\nu_{95,96}$	CH str.	3030.71	0.000
$\nu_{97,98}$	ring (CC str.) (circumference) + δCH (sciss.)	1504.60	0.000
$\nu_{99,100}$	δCH (scissoring)	1418.32	0.000
$\nu_{101,102}$	ring (CC str.)	1322.60	0.000
$\nu_{103,104}$	δCH (scissoring) +δring (δCCC)	1217.29	0.000
$\nu_{105,106}$	δring (δCCC) + δCH (scissoring)	1026.64	0.000
$\nu_{107,108}$	γCH (twist.)	864.83	0.000
$\nu_{109,110}$	γring (γCCC) (puckering.)	742.32	0.000
$\nu_{111,112}$	γring (γCCC) (puckering.)	678.44	0.000
$\nu_{113,114}$	γring (γCCC) (puckering.)	483.87	0.000
$\nu_{115,116}$	γring (γCCC) (puckering) external edge	171.96	0.000
E_5			
$\nu_{117,118}$	CH str.	3030.69	0.000
$\nu_{119,120}$	ring (CC str.) (circumference) + δCH	1512.57	0.000
$\nu_{121,122}$	ring (CC str.)(axial) + δCH (rocking)	1435.91	0.000
$\nu_{123,124}$	δCH (rocking)	1279.57	0.000
$\nu_{125,126}$	δCH (rocking)	1151.61	0.000
$\nu_{127,128}$	δring (δCCC) elongation	959.57	0.000
$\nu_{129,130}$	γCH (wagging)	885.61	0.000
$\nu_{131,132}$	γring (γCCC) (puckering.)	726.15	0.000
$\nu_{133,134}$	γring (γCCC) (puckering.)	631.81	0.000
$\nu_{135,136}$	γring (γCCC) (puckering.)	481.57	0.000
$\nu_{137,138}$	γring (γCCC) (puckering.)	307.70	0.000

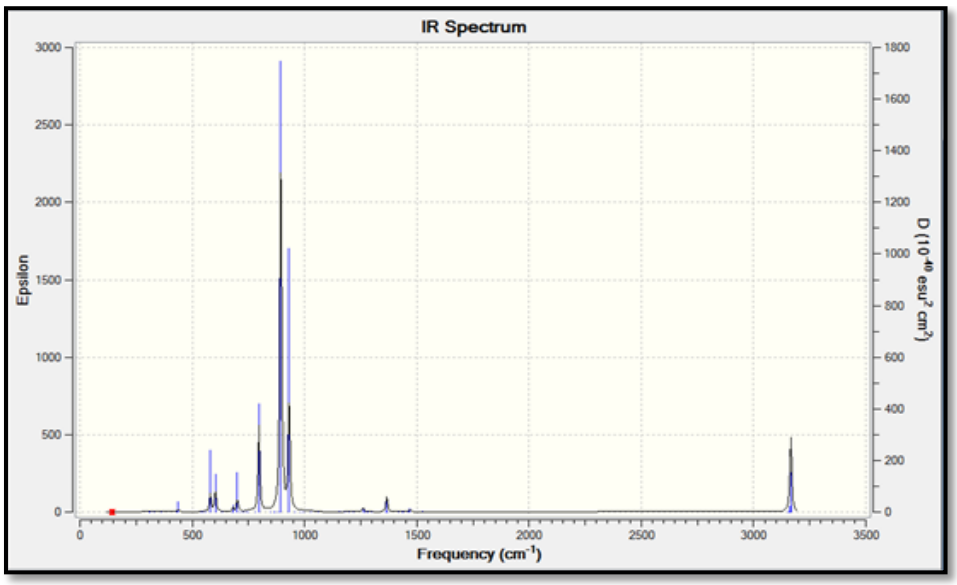

Figure 3. IR spectrum of Di-rings layer SWCNT as calculated applying DFT method.

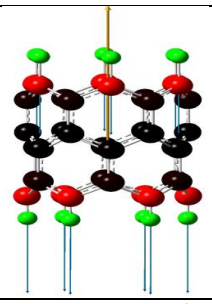	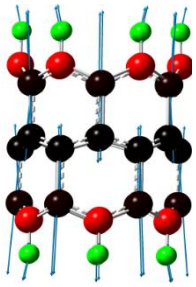	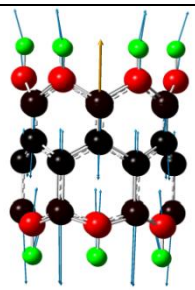	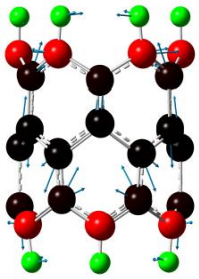
ν_{16}, 3040 cm^{-1} CH asym. str.	**ν_2, 1555 cm^{-1}** ring (CC str.) (axial)	**ν_{17}, 1468 cm^{-1}** ring (CC str.) (axial)	**ν_{47}, 1371 cm^{-1}** ring (CCC str.)
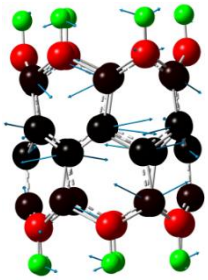	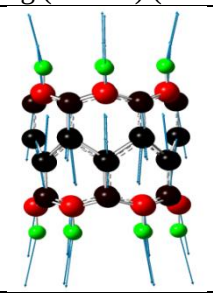	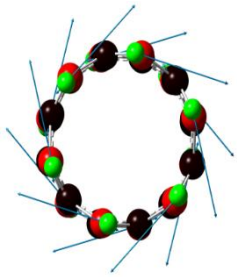	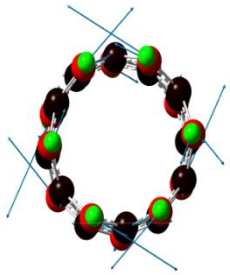
ν_{73}, 1360 cm^{-1} ring (CCC str.)(circum)	**ν_3, 1302 cm^{-1}** δring (δCCC) elongation	**ν_{14}, 1182 cm^{-1}** δCH (clock-anti clock)	**ν_{105}, 1027cm^{-1}** δring (δCCC)
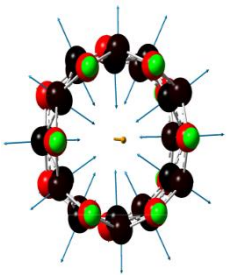	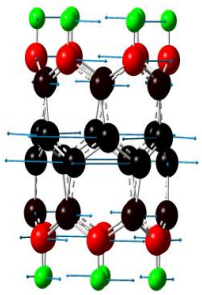	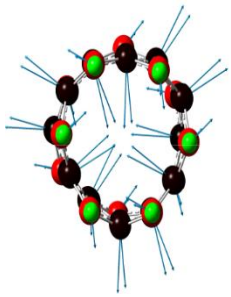	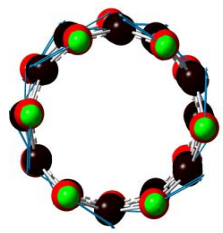
ν_{20}, 701cm^{-1} γCCC (puckering)	**ν_{15}, 561 cm^{-1}** δring (δCCC) clock-anti clock	**ν_{89}, 364 cm^{-1}** γring (γCCC) (puckering)	**ν_{12}, 328 cm^{-1}** δCCC (clock-anti clock)

Figure 4. Images of some modes of vibration for the calculated Di-RL (6, 0) zigzag SWCNT using, Gaussian 09 program.

- Vibration Frequency Assignment for the Tetra Rings-layer (6,0) Zigzag SWCNT ($C_{60}H_{12}$)

The Tetra-ring layers zigzag SWCNT posses 210 fundamental vibrations. Inspection of its irreducible representations, as defined by the symmetry character table (23).The results were shown for the following modes of vibration;

$\Gamma_{vibration}= \Gamma_{total} - (\Gamma_{rotation}+ \Gamma_{translation}) = 3N-6= 216-6= 210= 12A_1+ B_1+5A_2+ 11B_2+ 17E_1+ 18E_2+ 18E_3 +18E_4+ 17E_5$

These are 75 modes of vibration in number, of which 47 are Raman active ($12A_1$ (polarized) + $18E_2$ (depolarized) $+17E_5$ (depolarized), and 28 IR active ($11B_2 + 17E_1$).

- νCH Stretching Vibrations

There are 12 CH stretching vibrations according to number of CH bonds. The range of the frequency values is (3001-3050cm^{-1}), showing the following correlations:

$\nu_{sym.}$CH $_{str.}$(3050.17 cm^{-1}) (A_1) > $\nu_{asym.}$CH $_{str.}$ (3050.04 cm^{-1}) (B_2)

The highest intensity is 65.390 km/mol due to ν_{24}(3050.04 cm^{-1}) (B_2).

In general:**$\nu_{sym.}$CH $_{str.}$> ν_{asym}CH $_{str.}$**

-ν(C--C) Stretching Vibrations

The range of the calculated C--C stretching vibration is (1260-1573cm^{-1}), shown in the following correlations;

$\nu_{sym.}$(C--C $_{str.}$) (1573 cm^{-1}) (axial.)(A_1) >$\nu_{asym.}$(C--C $_{str.}$) (1562 cm^{-1}) (axial.) (B_2)

$\nu_{sym.}$(C--C $_{str.}$) (1573 cm^{-1}) (axial.)(A_1) >$\nu_{asym.}$(C--C $_{str.}$) (1513 cm^{-1})(circum.) (E_5)

$\nu_{sym.}$(C--C $_{str.}$) (1573 cm^{-1}) (axial.) (mid rings)(A_1) >$\nu_{sym.}$(C--C $_{str.}$) (1527cm^{-1}) (axial) (outer rings) (A_1)

In general: **$\nu_{sym.}$ (C--C $_{str.}$) >$\nu_{asym.}$ (C--C$_{str.}$)**

The highest intensity is 584.722 km/mol due to ν_{44}(1404 cm^{-1}) (E_1).

-νRing (C--C--C) Stretching Vibrations

The vibration of these modesare not located at definite C atoms like **ν(CC)** as could be seen from the atomic displacement vectors**,** Figure 2. According to their assignment, they were fallen in the range of (1216-1516 cm^{-1}).

ν_{asym}(C--C--Cstr.)(1516 cm^{-1}) (axial)(E_5)>$\nu_{asym.}$(C--C--Cstr.) (1513cm^{-1})(circum.)(E_5)

The highest intensity is 62.722 km/mol due to $\nu_{40,41}$ (1478cm^{-1}) (E_1).

In Plane (of the Tube) CH Deformation Vibrations (δCH)

Their displacement vectors are mainly located at the corresponding H atoms. The range of the calculated frequency values is (1055-1443 cm^{-1}).

$(\delta CH)_{asym.}$ scissoring (1443 cm^{-1}) (E_3) > $(\delta CH)_{asym.}$ clock-anticlock) (1437 cm^{-1}) (B_1)

$(\delta CH)_{asym.}$ scissoring (1494 cm^{-1}) (E_4) > $(\delta CH)_{asym.}$ rocking (1256 cm^{-1})(E_1)

The highest intensity is17.708 km/mol due to $\nu_{48,49}$ (1256 cm^{-1}) (E_1).

In Plane (of the Tube) Deformation Vibrations (δC--C--C)

The (δ**C--C--C**) vibrations are of smaller values than **δCH**. According to their assignment, they were fallen in the range (209-1297 cm^{-1}). These mode include the expected clock and anticlockwise, elongation vibration motions, also showing the following relations;

$(\delta C\text{--}C\text{--}C)_{sym.}$(elongation)(1297cm^{-1}) (A_1)> $(\delta C\text{--}C\text{--}C)_{asym.}$(elongation)(1150 cm^{-1}) (B_2)

The highest intensity is 5.039 km/mol due to ν_{30} (650 cm^{-1}) (B_2).

Out of Plane (of the Tube) Deformation Vibration Frequencies (γCH)

-The range of the (γCH) vibration frequenciesis (798-904cm^{-1}). The following relations hold too;

(γCH) $_{sym.}$ (904cm^{-1}) (wagging) (A_1) > $(\gamma CH)_{asym.}$(893 cm^{-1}) (wagging) (B_2)

(γCH) $_{sym.}$(904cm^{-1}) (wagging) (A_1) > $(\gamma CH)_{asym.}$(856 cm^{-1}) (twisting) (E_4)

The highest intensity is 179.346 km/mol due to $\nu_{54,55}$ (835 cm^{-1}) (E_1).

-γRing out of Plane (of the Tube) Deformation Vibrations (γC--C--C)

The range of the vibration frequencies for the (γ**C--C--C**) is (152-819 cm^{-1}). The modes include breathing, and puckering deformation modes of the whole ring. The relation of asymmetric to symmetric modes is viewed in the following relation;

$(\gamma C\text{--}C\text{--}C)_{asym.}$ (puckering) (819 cm^{-1}) (E_1) > $(\gamma C\text{--}C\text{--}C)_{sym.}$(breathing) (727 cm^{-1}) (A_1)

The highest intensity is 100.250 km/mol due to ν_{33} (461 cm^{-1}) (B_2).

Table 3 shows the vibration frequencies assignment (3N-6) and absorption intensities of active IR absorption intensities of the Tetra-RLSWCNT.

Figure 5 shows the IR spectrum for the Tetra-RLSWCNT as calculated applying DFT method.

Figure 6 shows the images of some vibration modes for the calculated Tetra-RL using Gaussian 09 program.

Table 3. Vibration frequencies assignment (3N-6) and absorption intensities of the active IR modes for the Tetra-RL (6,0) zigzag SWCNT.

Symmetry & description		DFT (6-311G/ B3LYP)	
		Freq. (cm^{-1})	Intensity (km/mol)
A_1			
ν_1	CH str.	3050.17	0.000
ν_2	ring (CC str.) (axial) mid.	1573.34	0.000
ν_3	ring(CC str.) (axial) outer	1526.85	0.000
ν_4	δring (δCCC) elongation	1297.02	0.000
ν_5	δring (δCCC) elongation	917.81	0.000
ν_6	γCH (wag.)	904.03	0.000
ν_7	γring (γCCC) breathing	727.13	0.000
ν_8	γring (γCCC) breathing	698.79	0.000
ν_9	γring (γCCC) breathing	522.12	0.000
ν_{10}	γring (γCCC) breathing	474.02	0.000
ν_{11}	γring (γCCC) outer	418.71	0.000
ν_{12}	δring (δCCC) elongation	320.45	0.000
B_1			
ν_{13}	δCH (clock-anti clock) + δring	1437.28	0.000
ν_{14}	δCH (clock-anti clock) + δring	1371.39	0.000
ν_{15}	Ring str. (CC str.) circum. + δCH(rock.)	1259.78	0.000
ν_{16}	δCH (clock-anti clock)	1148.48	0.000
ν_{17}	δring (δCCC) clock-anti clock	536.07	0.000
ν_{18}	δring (δCCC) clock-anti clock	208.79	0.000
A_2			
ν_{19}	δCH (clock-anti clock) + δring	1417.28	0.000
ν_{20}	δCH (clock-anti clock) + δring	1313.87	0.000
ν_{21}	δCH (clock-anti clock)	1149.00	0.000
ν_{22}	δring (δCCC) clock-anti clock mid	635.98	0.000
ν_{23}	γring (γCCC) (puckering)	392.11	0.000
B_2			
ν_{24}	CH str.	3050.04	65.390
ν_{25}	ring (CC str.) (axial)	1561.57	**367.437**
ν_{26}	ring (CC str.) (axial)	1457.54	44.707
ν_{27}	δring (δCCC) (elongation)	1150.28	0.025
ν_{28}	γCH (wagging)	893.44	**101.677**
ν_{29}	γring (γCCC) (puckering)	745.40	2.085
ν_{30}	δring (δCCC) (elongation)	650.30	5.039
ν_{31}	γring (γCCC) (puckering)	636.55	7.176
ν_{32}	γring (γCCC) (puckering)	591.57	**69.467**
ν_{33}	γring (γCCC) (puckering)	461.31	**100.250**
ν_{34}	γring (γCCC) (puckering) outer	419.39	6.542
E_1			
$\nu_{35, 36}$	CH str.	3046.70	10.261
$\nu_{37, 38}$	ring (CC str.)	1505.86	36.991
$\nu_{39, 40}$	ring (CCC str.) + δCH (rocking)	1477.99	62.722
$\nu_{41, 42}$	ring (CC str.) (axial)	1417.50	13.351
$\nu_{43, 44}$	ring (CC str.) (axial)	1403.64	**584.722**
$\nu_{45, 46}$	ring (CC str.) (circumference)	1300.10	9.432
$\nu_{48, 48}$	δCH (rocking) + δring	1256.36	17.707
$\nu_{49, 50}$	δCH (rocking)	1169.82	3.587
$\nu_{51, 52}$	δring (δCCC) elongation	921.27	3.556
$\nu_{53, 54}$	γCH (wagging)	834.74	**179.345**
$\nu_{55, 56}$	γring (γCCC) (puckering)+γCH (wagging)	819.43	8.412
$\nu_{57, 58}$	γring (γCCC) (puckering)(axial) outer	651. 96	18.455
$\nu_{59, 60}$	γring (γCCC)(puckering)	632.27	40.451
$\nu_{61, 62}$	γring (γCCC) (puckering)	578.43	**90.228**

$\nu_{63,\ 64}$	γring (γCCC) (puckering)	430.69	3.856
$\nu_{65,\ 66}$	γring (γCCC) (puckering)	377.88	1.639
$\nu_{67,\ 68}$	γring (γCCC) (puckering)	207.87	1.926
E_2			
$\nu_{69,\ 70}$	CH str.	3042.18	0.000
$\nu_{71,\ 72}$	Ring(CCCstr.)(circum.)outer+ δCH (sciss.)	1481.76	0.000
$\nu_{73,\ 74}$	CC str. (axial) + δCH (scissoring)	1424.11	0.000
$\nu_{75,\ 76}$	ring (CCC str.)	1350.08	0.000
$\nu_{77,\ 78}$	CC str. (axial) + δCH (scissoring)	1312.88	0.000
$\nu_{79,80}$	δCH (scissoring) + δring (δCCC)	1216.32	0.000
$\nu_{81,82}$	δring (δCCC)	1182.03	0.000
$\nu_{83,84}$	δring (δCCC)	1078.35	0.000
$\nu_{85,86}$	δring (δCCC)	928.83	0.000
$\nu_{87,88}$	γCH (twisting)	847.11	0.000
$\nu_{89,90}$	γCH (twisting)	810.69	0.000
$\nu_{91,92}$	γring (γCCC) (puckering.)	728.06	0.000
$\nu_{93,94}$	γring (γCCC) (puckering.)	651.73	0.000
$\nu_{95,96}$	γring (γCCC) (puckering.)	589.85	0.000
$\nu_{97,98}$	γring (γCCC) (puckering.)	496.79	0.000
$\nu_{99,100}$	γring (γCCC) (puckering.)	414.62	0.000
$\nu_{101,102}$	γring (γCCC) (puckering) (circumference)	225.64	0.000
$\nu_{103,104}$	γring (γCCC) (puckering.)	-45.12	0.000
E_3			
$\nu_{105,\ 106}$	CH str.	3000.85	19.391
$\nu_{107,\ 108}$	δCH (scissoring)	1443.32	0.017
$\nu_{109,\ 110}$	ring (CCC str.) (circumference) mid	1330.83	0.000
$\nu_{111,\ 112}$	ring (CCC str.) (circumference) mid	1312.60	0.000
$\nu_{113,\ 114}$	ring(CCC str.) (circum.) mid+ δCH (sciss.)	1216.34	0.000
$\nu_{115,\ 116}$	δCH (scissoring) + δring (δCCC)	1055.44	0.000
$\nu_{117,\ 118}$	δring (δCCC)	942.40	0.000
$\nu_{119,\ 120}$	γCH (twisting)	836.30	0.000
$\nu_{121,\ 122}$	γring (γCCC) (puckering)	728.42	3.463
$\nu_{123,\ 124}$	γring (γCCC) (puckering) (axial)	726.67	0.000
$\nu_{125,\ 126}$	γring (γCCC) (puckering)	704.04	0.000
$\nu_{127,\ 128}$	γring(γCCC)(pucking) (axial) outer ring	668.75	0.000
$\nu_{129,\ 130}$	γring (γCCC) (pucking)(axial) mid ring	629.43	0.000
$\nu_{131,\ 132}$	γring (γCCC) (puckering)	615.47	0.000
$\nu_{133,\ 134}$	γring (γCCC) (puckering)	536.13	0.000
$\nu_{135,\ 136}$	γring (γCCC) (puckering)	520.10	0.000
$\nu_{137,\ 138}$	γring (γCCC) (puckering) mid ring	392.04	0.000
$\nu_{139,\ 140}$	γring (γCCC) (puckering)(axial) outer ring	332.18	0.000
E_4			
$\nu_{141,\ 142}$	CH str.	3042.63	0.000
$\nu_{143,\ 144}$	ring(CCC str.)(circum.)outer+ δCH (sciss.)	1494.00	0.000
$\nu_{145,\ 146}$	ring (CC str.)(circum.) mid + δCH (sciss.)	1455.65	0.000
$\nu_{147,\ 148}$	ring (CC str.) (circumference)	1391.52	0.000
$\nu_{149,\ 150}$	ring (CC str.)(axial) + δCH (scissoring)	1356.95	0.000
$\nu_{151,\ 152}$	δCH(sciss.)+ ring (CCC str.) (circum.) mid	1287.28	0.000
$\nu_{153,\ 154}$	δCH (scissoring)	1208.01	0.000
$\nu_{155,\ 156}$	δring (δCCC)	1135.34	0.000
$\nu_{157,\ 158}$	δring (δCCC)	969.99	0.000
$\nu_{159,\ 160}$	γCH (twisting)	855.54	0.000
$\nu_{161,\ 162}$	γCH (twisting)	797.80	0.000

$\nu_{163,\ 164}$	γring (γCCC) (puckering)(axial) mid	677.90	0.000
$\nu_{165,\ 166}$	γring (γCCC) (puckering)	654.68	0.000
$\nu_{167,\ 168}$	γring (γCCC) (puckering) mid	581.61	0.000
$\nu_{169,\ 170}$	γring (γCCC) (puckering) outer ring	515.46	0.000
$\nu_{171,\ 172}$	γring (γCCC) (puckering)(axial)	485.68	0.000
$\nu_{173,\ 174}$	γring (γCCC) (puckering) outer ring	339.50	0.000
$\nu_{175,\ 176}$	γring (γCCC) (puckering) outer ring	152.04	0.000
E_5			
$\nu_{177,\ 178}$	CH str.	3046.78	0.000
$\nu_{179,\ 180}$	ring (CCC str.) (axial)	1516.20	0.000
$\nu_{181,\ 182}$	ring (CC str.) (circumference) outer	1513.30	0.000
$\nu_{183,\ 184}$	ring (CCC str.) (axial)+ δCH (rocking)	1411.13	0.000
$\nu_{185,\ 186}$	ring (CCC str.) + δCH (rocking)	1383.44	0.000
$\nu_{187,\ 188}$	ring (CCC str.)	1382.63	0.000
$\nu_{189,\ 190}$	δCH (rocking)	1238.80	0.000
$\nu_{191,\ 192}$	δCH (rocking)+δring (δCCC)	1183.72	0.000
$\nu_{193,\ 194}$	δring (δCCC)	1108.50	0.000
$\nu_{195,\ 196}$	δring (δCCC)	942.40	0.000
$\nu_{197,\ 198}$	γCH (wagging)	847.63	0.000
$\nu_{199,\ 200}$	γring (γCCC) (puckering.)	792.04	0.000
$\nu_{201,\ 202}$	γring (γCCC) (puckering.)	646.24	0.000
$\nu_{204,\ 179}$	γring (γCCC) (puckering.)	556.87	0.0000
$\nu_{206,\ 179}$	γring (γCCC) (puckering.)	539.21	0.0000
$\nu_{208,\ 179}$	γring (γCCC) (puckering.)	348.80	0.0000
$\nu_{210,\ 179}$	γring (γCCC) (puckering.)	293.40	0.0000

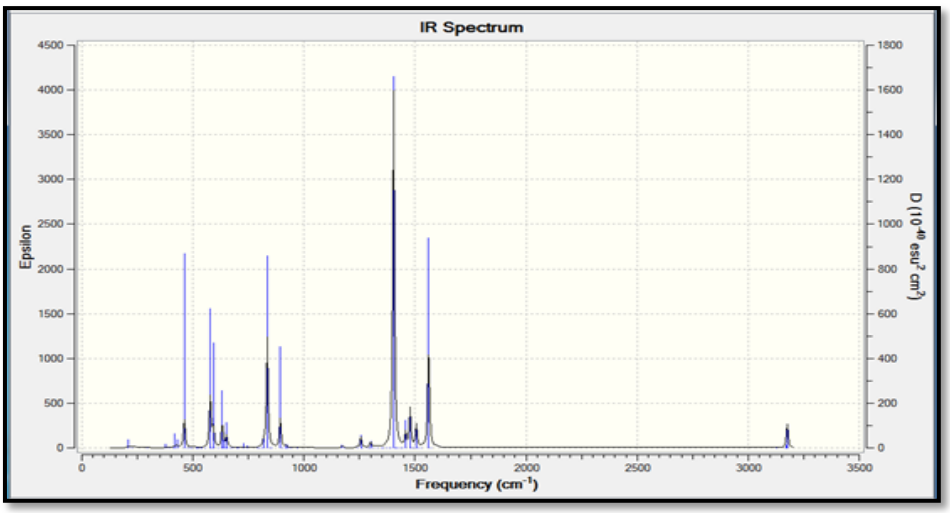

Figure 5. IR spectrum for Tetra-RL SWCNT as calculated applying DFT method.

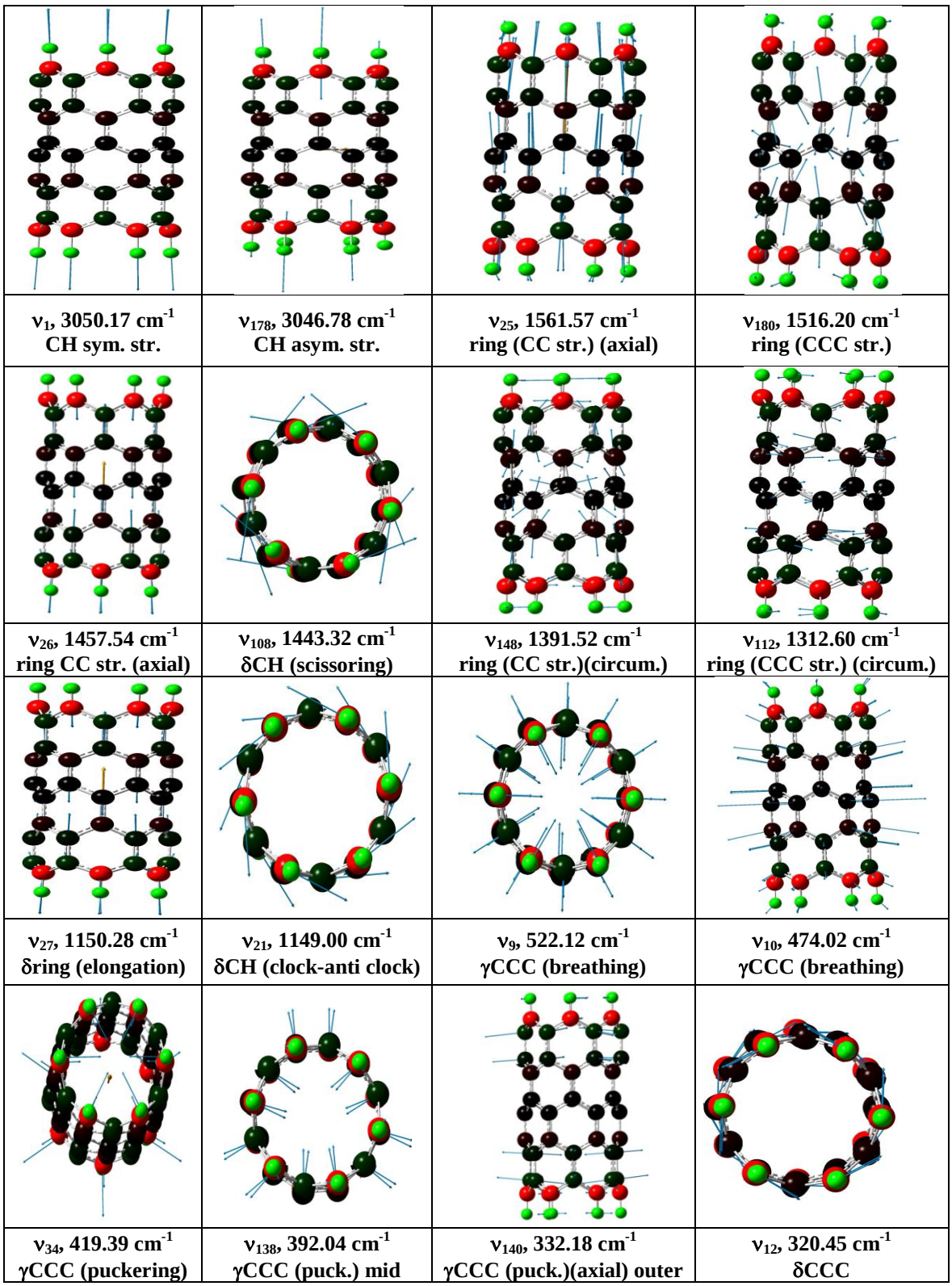

Figure 6. Images of some modes of vibration for the calculated Tetra-RL (6, 0) zigzag SWCNT using Gaussian 09 program.

Conclusion:

1-Quantum mechanical calculation method DFT (6-311G/B3LYP) was carried out for optimization of Di and Tetra-rings layers of (6,0) zigzag SWCNTs. Bothwere showed D_{6d} point group. Gaussian 09 program was used to investigate the assignment of (3N-6) mode of vibrations (IR active and Raman active) at minimize geometries.

2- Comparison of the geometry, physical properties, vibration frequency modes were done for the even-rings layer Di and Tetra-RL SWCNTs.

3-The finger print vibrations (basic vibrations) of Di and Tetra RLSWCNTs were measured and completely assigned such as δC--C--C (elongation and clock-anti-clockwise), (γCCC) (puckering, breathing),δCH (clock-anti clock, scissoring, rocking), and γCH

(wagging, twisting) deformation modes, which are directly related to the viability electronic conductivity.

Conflicts of Interest: None.

References:

1. Vasic B, Kratzer M, Matkovic A, Nevosad A. Ralevi U, Jovanovic D, et al. Atomic force microscopy based manipulation of graphene using dynamic plowing lithography. Nano. Tech. 2013;24(1):015303-9.
2. Jorio A, Piment MA, Filho AG, Saito R, Dresselhaus G, Dresselhaus MS. Characterizing carbon nanotube samples with resonance Raman scattering. New J. Phys. 2003; 5(139):1-17.
3. Wissam AS, Norman P. Probing single-walled carbon nanotube defect chemistry using resonance Raman spectroscopy. Carbon. 2014**;**67:16-26**.**
4. Natsuki T, Melvin GJ. Vibrational frequencies and Raman radial breathing modes of multi-walled carbon nanotubes based on continuum mechanics. J. Mat. Sci. Res. 2013**;**2(4):0585-0592.
5. Kahidan A, Shirmohammadian M. Properties of carbon nanotube (CNT). Inter. J. Eng. 2016;5(6):497-503.
6. Harris PJ. Carbon Nanotubes and Related Structures, Cambridge University Press, Cambridge, 1999.
7. Babu KS, Murthy KSR, Kumar EK. Axial compression based hyper elastic modeling of buckling response in single wall carbon nanotubes. Inter. J. Eng. Scie. Inven. 2013**;**2(5):1-4.
8. Zidour M, Daouadji TH, Benrahou KH, Tounsi A, Adda BA, Hadji L. Buckling analysis of chiral single-walled carbon nanotubes by using the non local Timoshenko beam theory. Mech. Compos. Mat. 2014;50(1):95–104.
9. Yan y, Weizhong Li, Wang W. The effect of wettability on the dynamical behaviors of single-walled carbon nanotube. Sage j. 2014;7(1):1567–1579, b) Yan Y, Wenquan W, Lixiang Z. Free vibration of the fluid-filled single-walled carbon nanotube based on a double shell-potential flow model. App. Math. Mod. 2012;36(12);6146-6153.
10. Gupta AK, Harsha SP. Analysis of mechanical properties of carbon nanotube reinforced polymer composites using continuum mechanics approach. Procedia Mater. Scie. 2014;6:18-25.
11. MuhammadI D, Awang M, Seng LK. Numerical modelling of Young's modulus of single-layered cubic zirconia nanosheets. Advan. Struc. Mater. 2015;70:373-380.
12. Kubba RM, AL-Ani HN, Shanshal M. The vibration frequencies of [6] cyclacenes (linear, angular and angular-chiral) mono ring molecules. Jordan j. Chem. 2011**;**6(3):269-290.
13. Kubba RM, Samawi KA. Theoritical study of electronic properties and vibration frequencies for Tri-Rings Layer (6,0) linear (zigzag) SWCNT. Iraq. J. Sci. 2014;55(2B):606-616.
14. Kubba RM, Samawi KA. Theoretical study of bonds length, energetic and vibration erequencies for construction units of (6,0) ZigZag SWCNTs. Iraq. J. Sci. 2015;56(3A):1821-1835.
15. Kubba RM, AL-Ani HNA. DFT treatments for studying the vibration frequencies and normal coordinates of cyclacene molecules with different diameters (unit construction of zigzag SWCNTs). Iraq. J. Phys. 2012;10(18)**:**135-146.
16. Kubba RM, AL-Ani HN. Comparison study of CC and CH vibration frequencies and electronic properties of mono, Di, Tri, and Tetra-Rings Layer of arm chair (SWCNTs). Iraq. j. Phys. 2013;11(20):85-99.
17. Andzelm JW, Labanowski JK. Density Functional Methods in Chemistry, Springer-Verlag, NewYork, 1991.
18. Goerigk L, Grimme S. Double-hybrid density functional, computational molecular science, 2014;4(6):576-600.
19. Rong H, Huang Yi, Heng Xu. Comment on synthesis and characterization of the pentazolate anion cyclo-N_5– in $(N_5)_6(H_3O)_3(NH_4)_4Cl$. Sci. J. 2018;359:6381.
20. Lewars E. COMPUTATIONAL CHEMISTRY. Introduction to the Theory and Applications of Molecular and Quantum Mechanics. Chemistry Department, Trent University, Peterborough, Ontario, Canada, 2003.
21. Frisch MJ, Pople JA. Gaussian 09, Revision E.01. Gaussian, Inc., Wallingford CT. 2009.
22. Jorio A, Saito R, Hafner JH, Liebre CM, Hunter M, Mcclur T, Dresselhaus G. Structural (n,m) determination of isolated single–wall carbon nanotubes by resonant Raman scattering. Phys. Rev. Lett. 2001;86 (6):1118-1121.
23. Davidson G. Introduction to Group Theory for Chemists. Applied Science Publishers Ltd. London, Elsevier Publishing Comp. Ltd. 1990.
24. Lee JB, Balikov DA, Yang JW, Kim KS, Park HK, Kim JK, etal. Cationic Nanocylinders Promote Angiogenic Activities of Endothelial Cells. Polymers (Basel). 2016**;**8(15): 1-11.
25. Odom TW, Huang J, Kim P, Lieber CM. Structure and electronic properties of CNT. J. Phy. Chem. 2000;104(13):2794-2809.
26. Vitali L, Bughard M, Schneider MA, LeiLiu YWu, Jayanthi CK. Phonon spectromicroscopy of carbon nanostructures with atomic resolution, Max Planck Institute for Sol. St. Res. Lett., 2004**;**93(13):136103-1-136103-4.
27. Kuhlman U, Jantoljak H, Pfander N, Bernier P, Journet C. Thomsen C. Infrared active phonons in single-walled carbon nanotubes, Chem. Phys. Lett., 1998**;**294(1-3):237-240.
28. Burghard M. Electronic and vibrational properties of chemically modified (SWCNTs), Surface Science Reports. Max-plank-Institutfuer, Germany, 2005**;**58(4):1-5.
29. Alon OE. Number of Raman and infrared-active vibrations in single-walled carbon nanotubes. Physical Review. 2001**;**B63(20):201403-1-201403-3.
30. Herzberg G. Molecular Spectra and Molecular Structure, Infrared and Raman spectra of Polyatomic Molecules. Van Nostrand Co, New York, 1971.

الشكل الهندسي وترددات وانماط الاهتزاز والإحداثيات المتعامدة بعدد (3N-6) وشدة امتصاص الأشعة تحت الحمراء لانبوبي نانوكاربون ثنائي و رباعي الطبقة الحلقية نوعSWCNT (Zigzag) (6, 0)

رحاب ماجد كبة **خالدة عبيد سماوي**

قسم الكيمياء، كلية العلوم، جامعة بغداد، بغداد، العراق.

الخلاصة:

تضمن البحث استخدام طريقة حساب نظرية دوال الكثافة DFT نوع (B3LYP) بعناصر قاعدة (6-311G) و باستخدام برنامج Gaussian-09 في حساب الشكل الهندسي التوازني لانبوبي نانوكاربون نوع زكزاك ثنائي ورباعي الطبقة الحلقية اللذان وجد امتلاكهما لنفس التماثل وفق نظرية المجموعة D_{6d} وبتعاقب جميع اواصر CC سواء كانت الاواصر العمودية C—Ca (باتجاه المحور z) أو الاواصر المحيطية C—Cc (الحافة الخارجية و لوسط الانبوب). تم تصنيف ترددات اهتزاز طيف الأشعة تحت الحمراء وبعدد (3N-6) وتشخيصها تكافؤيا و تماثلياعتمادا على اشكال الانماط التي تم الحصول عليها باستخدام عرض برنامج Gaussian 09. وتم ايجاد جميع العلاقات المتعلقة بالانماط المختلفة كترددات مط νCH و νC--C وترددات الانحناء δCH وC—C--δ و γCH و γC—C و γC--C--C، المتضمنة الحركات التنفسية والانبعاجية الانحنائية باتجاه وبعكس اتجاه عقرب الساعة.

الكلمات مفتاحية: انبوب ثنائي و رباعي الطبقة، شدة الامتصاص، الاحداثيات المتعامدة، الانماط الاهتزازية، SWCNT، ، ترددات الاهتزاز،